Unsupervised Brain Computer Interface Based on Intersubject Information and Online Adaptation

Shijian Lu, *Member, IEEE*, Cuntai Guan, *Senior Member, IEEE*, and Haihong Zhang

***Abstract*—Conventional brain computer interfaces rely on a guided calibration procedure to address the problem of considerable variations in electroencephalography (EEG) across human subjects. This calibration, however, implies inconvenience to the end users. In this paper, we propose an online-adaptive-learning method to address this problem for P300-based brain computer interfaces. By automatically capturing subject-specific EEG characteristics during online operation, this method allows a new user to start operating a P300-based brain–computer interface without guided (supervised) calibration. The basic principle is to first learn a generic model termed *subject-independent model* offline from EEG of a pool of subjects to capture common P300 characteristics. For a new user, a new model termed *subject-specific model* is then adapted online based on EEG recorded from the new subject and the corresponding labels predicted by either the subject-independent model or the adapted subject-specific model, depending on a confidence score. To verify the proposed method, a study involving 10 healthy subjects is carried out and positive results are obtained. For instance, after 2–4 min online adaptation (spelling of 10–20 characters), the accuracy of the adapted model converges to that of a fully trained supervised subject-specific model.**

***Index Terms*—Brain–computer interfaces (BCIs), event related potential, online model adaptation, P300-based word speller.**

I. Introduction

THE emerging technology of brain–computer interfaces (BCIs) has attracted increasing interests from multidisciplinary domains [1]–[4]. Currently, user calibration is still an important part of electroencephalography (EEG)-based BCIs because of considerable variations across subjects [5]–[7]. Take mu–beta control as an example. The mu–beta training in [5] requires each subject to participate in three training sessions per week where each training session takes around 30 min and the whole training process lasts up to 6–8 weeks.

A typical user calibration procedure often starts with a user preparation stage during which an electrode cap is attached and a user briefing is conducted including the introduction of the experiment protocol and the delivery of the detailed instructions to be followed. After that, a certain amount of subject EEG is collected during the user calibration process, which can then be used to build a subject-specific classification model (SSCM). The learned SSCM can be further used to classify the future EEG of the subject under study. However, the user calibration renders most existing BCIs inconvenient for practical uses.

Manuscript received May 12, 2008; revised September 08, 2008; accepted November 05, 2008. First published February 18, 2009; current version published April 08, 2009.

The authors are with the Institute for Infocomm Research, 138632, Singapore (e-mail: slu@i2r.a-star.edu.sg; ctguan@i2r.a-star.edu.sg; hhzhang@i2r.a-star.edu.sg).

Digital Object Identifier 10.1109/TNSRE.2009.2015197

Fig. 1. Interface of a P300-based word speller: Six rows and six columns shown above flash alternatively in a random order during each flashing round. A P300 event-related potential (ERP) will be elicited when the row or the column specifying the focused cell flashes. The row and the column specifying the focused cell can be determined through the identification of P300 ERP within the EEG recorded during the flashing process.

A number of methods have been reported to speed up the user calibration process. For example, Blankertz *et al.* [6] propose to reduce the training data for motor imagery through the regularization of the covariance matrix that needs to be evaluated for Fisher's linear discriminant. Li *et al.* [8], [9] propose to reduce the training data through self-training that first learns a weak classifier from a small amount of labeled data and then improves the weak classifier based on unlabeled data and corresponding labels predicted by the weak classifier itself. However, it is still an open question to use BCIs directly without the user calibration.

This paper presents the first attempt to address this issue for P300-based BCIs. It extends and consolidates our earlier work [10] on preliminary research of adaptive P300-based BCIs. In particular, this paper reports an online model adaptation technique that makes use of EEG of other subjects and allows use with no training for a new subject. Before introducing the methodology, we would like to give a brief overview of prior work on P300 and P300-based BCIs (more specifically on P300-based word spellers).

P300 is an endogenous event-related potential (ERP) which presents as a positive deflection at a latency of around 300 ms after the onset of external stimuli [11], [12]. Farwell and Donchin [13] first demonstrate the use of P300 for BCIs in a so-called oddball paradigm. In that paradigm, the computer displays a matrix of cells shown in Fig. 1 representing different letters and flashes rows and columns round by round. In each flashing round the six rows and the six columns flash one time alternately in a random order. Subjects trying to spell a character need to focus on the related cell visually for a short while, meanwhile a P300 ERP will be elicited when the row or the column specifying the focused cell flashes. The elicited P300

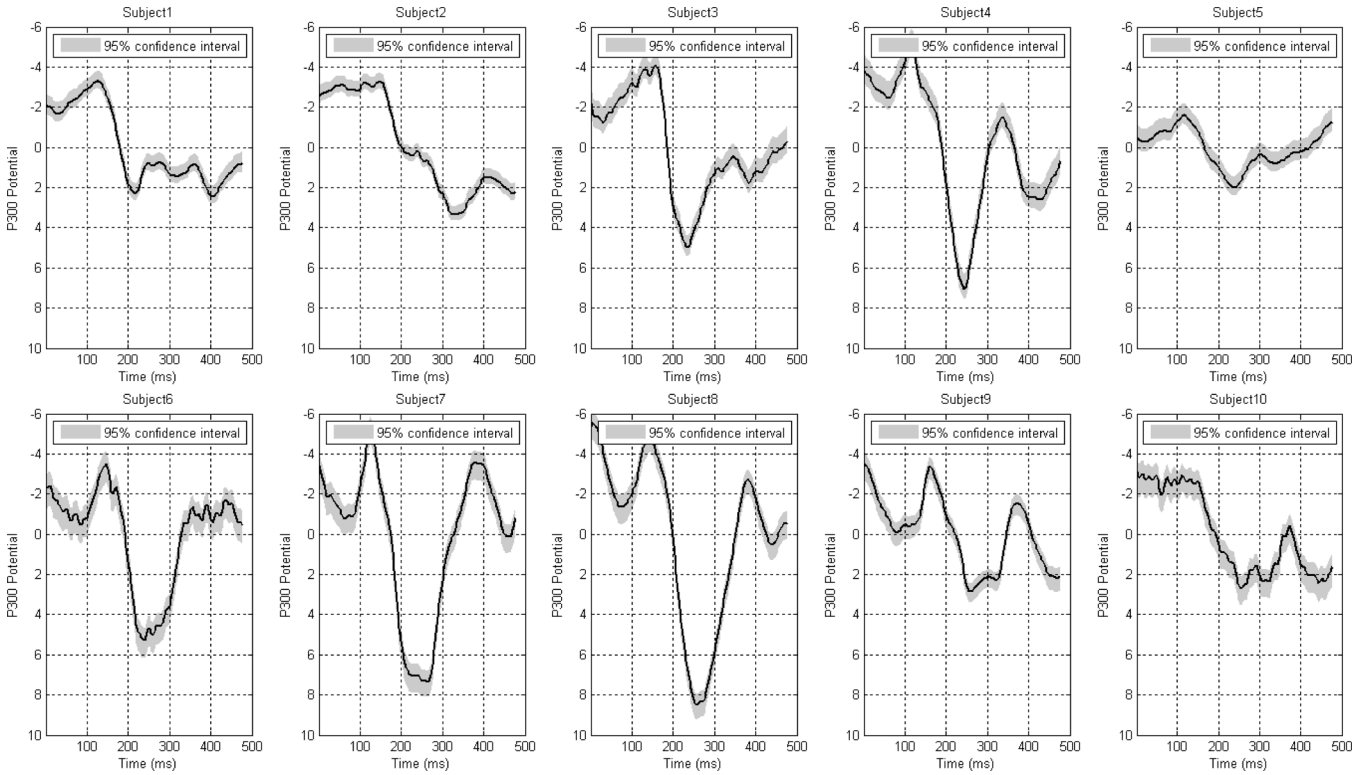

Fig. 2. P300 event-related potential of ten healthy subjects under study: P300 is measured at channel Cz where x axis gives the time from the stimulus onset and the P300 curves are derived by averaging 820 EEG trials with P300 (41 characters $\times$ 10 rounds $\times$ 2 flashes including one row flash and one column flash that specify the focused cell). The gray area in each subfigure shows the 95% confidence interval with sample size at 820.

can then be identified by certain machine learning algorithms [7], [14]–[18].

Many studies [19]–[21] have shown that P300 varies across subjects as illustrated in Fig. 2 where P300 of ten healthy subjects is calculated through averaging 820 EEG trials with P300. In particular, P300 amplitude and latency vary among both normal and clinical populations. Such cross-subject variations are found to be closely related to the background EEG activity [22] and have been linked to individual differences in cognitive capability. Due to the P300 variations across subjects, a computational P300 classification model learned from EEG of one subject usually would not apply well to classify EEG of another subject [23].

This paper presents an online model adaptation technique that makes use of EEG of other subjects and allows zero user calibration. To the best of our knowledge, this is the first attempt to adapt a SSCM online so that a new user can directly use P300-based BCIs without the user calibration. The proposed technique is based on three observations [20], [22], [23] including: 1) P300 of the same subject is pretty consistent within a short period (say, 5–10 h), though it may vary after a long period of time such as aging; 2) P300 of different subjects shares common waveform characteristic as defined, namely, a positive peak at channels such as Cz shown in Fig. 2 after around 300 ms of the onset of external stimuli; 3) P300 usually varies across subjects in terms of the peak amplitude and the peak latency.

Fig. 3 shows the framework of our proposed technique. First, an EEG model is built offline to capture common P300 characteristics by learning from EEG of a pool of subjects. Such model will be uniformly referred by subject-independent classification model (SICM) later because it is learned from EEG of a pool of subjects and so independent of any specific subject. Starting from the SICM, we further derive a SSCM through an online adaptation process. In particular, EEG from a new subject is first classified by the SICM at the initial adaptation stage. A subject-specific model is then built based on the classified subject EEG and the corresponding labels predicted by the SICM. After that, the newly built subject-specific model is iteratively updated through the incorporation of the ensuing EEG of the new subject and the corresponding labels predicted by either itself or the SICM, depending on a confidence score. In the ensuing discussions, we uniformly denote the adapted SSCM (by our proposed method) and supervised SSCM (learned from labeled subject EEG) by using ASSCM and SSSCM, respectively.

The rest of this paper is organized as follows. Section II first presents the proposed EEG classification technique. Section III then evaluates the proposed technique by using EEG collected from ten healthy subjects. After that, the proposed technique is discussed in Section IV. Some concluding remarks are finally drawn in Section V.

II. Proposed EEG Classification Technique

This section presents our proposed EEG classification technique. In particular, we will divide this section into three subsections, which deal with the EEG preprocessing and classification by Fisher's linear discriminant, the subject-independent EEG modeling and classification, and the adaptive EEG modeling and classification, respectively.

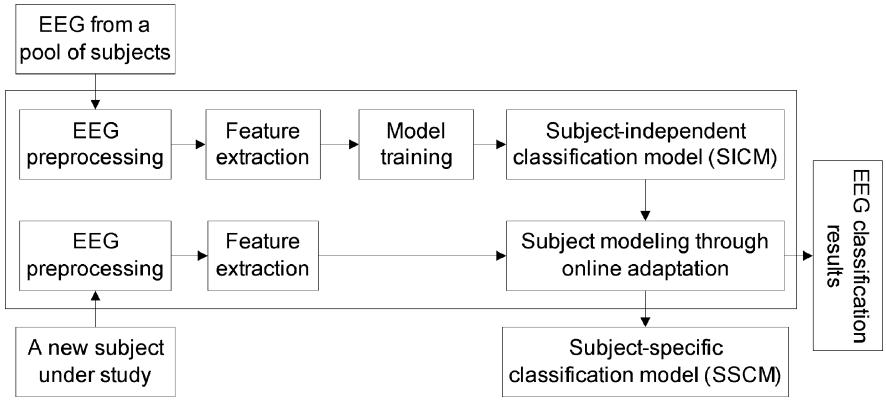

Fig. 3. Framework of the proposed EEG modeling and classification technique: A subject-independent classification model is first learned from EEG of a pool of subjects. Starting from the SICM, a subject-specific model is then derived through the adaptation of subject EEG recorded online.

A. EEG Preprocessing and Classification

Subject EEG $E(n)$ recorded in each epoch (EEG segment between 150–500 ms following an external stimulus) needs to be preprocessed before its classification. In the proposed technique, each epoched EEG $E(n)$ is first fed to a low-pass filter and then down-sampled at 60 Hz with sampling rate at 250 Hz. Such down-sampling reduces the data size and at the same time speeds up the ensuing EEG processing significantly. After that, the epoched EEG $E(n)$ is further filtered by a ten-order Chebyshev II type IIR filter where the passband cutoff frequency is set at 10 Hz as described in [24].

Ocular artifacts are then removed by treating each epoched EEG $E(n)$ as a linear superposition of the electrooculograph (EOG) $U(n)$ and the real EEG $X(n)$ as follows [25], [26]:

$$E(n) = \sum_{i=1}^{N} b_i U_i(n) + X_i(n) \tag{1}$$

where N is the number of sites at which the EOG is measured, two in our setup. Since the dynamic range of X is small in comparison to U, the propagation constants b_i can be computed through the least square minimization. The model in (1) assumes that the real EEG $X(n)$ is uncorrelated, which cannot be satisfied in real situations. To relax this assumption, a difference model for the artifact propagation can be assumed as follows:

$$E(n) = E(n-1) + \sum_{i=1}^{N} b_i(U_i(n) - U_i(n-1)) + X_i(n) - X_i(n-1). \tag{2}$$

The difference model in (2) follows from the one in (1), which removes the intersample correlations of the required EEG $X(n)$. Our experiments show that the difference model consistently outperformed the one in (1). We therefore remove ocular artifacts by using the difference model throughout the study reported here.

In an oddball paradigm, 12 flashes intensify in a random order within each flashing round where one row flash and one column flash specifying the focused cell have P300 and the rest has no P300. Therefore, EEG classification in P300-based BCIs is actually a two-class classification problem. To facilitate the ensuing EEG classification, we first concatenate the preprocessed EEG from different channels into an EEG feature vector as follows:

$$X = \left[x_1^T, \ldots, x_i^T, \ldots, x_h^T\right]^T \tag{3}$$

where x_i refers to the preprocessed EEG segment that is recorded from the ith channel. Parameter h refers to the number of channels selected (8 channels in our setup).

Practically, we approximate the distribution of the converted EEG feature vector X in (3) by a multivariate Gaussian distribution as follows:

$$p(X|\pi_c) = \frac{1}{(2\pi)^{p/2}|\Sigma_c|^{1/2}} \exp^{-(1/2)(X-\mu_c)^T \Sigma_c^{-1}(X-\mu_c)}, \quad c = 1, 2 \tag{4}$$

where X refers to the EEG feature vector converted from the preprocessed EEG and p is equal to the dimension of X. In the proposed technique, we define two classes, namly, $c = 1$ and $c = 2$ to represent the mode of EEG trials with and without P300, respectively. Therefore, parameters μ_c and Σ_c, $c = 1, 2$ in (4) refer to the mean and the covariance matrix of EEG feature vectors with and without P300.

Different EEG classification techniques have been reported for P300-based word spellers. As evaluated in [27], support vector machine (SVM) and Fisher's linear discriminant (FLD) outperforms others in most cases. We design an EEG classifier based on FLD because of its lower computational cost compared with SVM. In particular, FLD attempts to find a linear vector w to project a high-dimensional feature into a 1-D feature so that the ratio between the projected between-class and within-class variance is maximized

$$\underset{w}{\operatorname{argmax}} J(w) = \frac{w^T S_b w}{w^T S_w w} \tag{5}$$

where S_b and S_w correspond to the between-classes scatter matrix and within-classes scatter matrix that can be evaluated as follows [28]:

$$S_b = \sum_c N_c(\mu_c - \overline{X})(\mu_c - \overline{X})^T$$
$$S_w = \sum_c \sum_{i \in c} (X_i - \mu_c)(X_i - \mu_c)^T, c = 1, 2 \tag{6}$$

where N_c and μ_c denote the number and the mean of samples in class c, respectively. $\overline{X}$ refers to the mean of samples within all two classes (EEG with and without P300). The linear projection vector w in (5) can be estimated by $w = \Sigma^{-1}(\mu_1 - \mu_2)$ [28].

As the EEG feature vector X has a normal distribution, the linear vector w can also be determined by the discriminant function evaluated by the posterior probability as follows [29]:

$$\begin{aligned} g_c(X) &= \ln p(X|\pi_c) + \ln p(\pi_c) \\ &= X^T\Sigma_c^{-1}\mu_c - \frac{1}{2}\mu_c^T\Sigma_c^{-1}\mu_i + \ln p(\pi_c), c = 1, 2 \end{aligned} \quad (7)$$

where π_c, $c = 1, 2$ denote two hypotheses of EEG feature vectors with and without P300, respectively. The quantity $p(\pi_c)$, $c = 1, 2$ refer to the prior probability of the two classes. According to the protocol of P300-based word spellers, $p(\pi_c)$, $c = 1, 2$ is equal to 1/6 and 5/6, respectively, for EEG trials with and without P300. The distribution parameters μ_c and Σ_c, $c = 1, 2$ can be estimated from EEG feature vectors that are converted from the training data. In practice, EEG feature vectors with and without P300 are approximated to have the same covariance matrix (i.e., $\Sigma_1 = \Sigma_2$).

P300 can thus be identified based on the discriminant evaluated in (7). Due to various types of noise within the collected subject EEG, most P300-based word spellers usually record multiple rounds of subject EEG and identify P300 by averaging the discriminant of EEG collected in each round. To combine the discriminant of multiple rounds of subject EEG properly, we first normalize the discriminant evaluated in (7) to a pair of numbers that represent the probability of EEG with and without P300 as follows:

$$g'_c = \frac{\exp(g_c - \min(G))}{\sum_{c=1}^{2}\exp(g_c - \min(G))}, c = 1, 2 \quad (8)$$

where $G = [g_1, g_2]$ corresponds to the discriminant of EEG with and without P300, respectively. Function $\min()$ returns the mimimum of the discriminant vector G. Clearly, the minus of the $\min()$ followed by a division operation in (8) converts the discriminant g_c, $c = 1, 2$ into a pair of numbers (i.e., g'_c, $c = 1, 2$ that represent P300 and non-P300 probabilities) that lie between 0 and 1 and at the same time sum up to 1 (i.e., $g'_1 + g'_2 = 1$).

P300 can thus be identified by the row and the column that have the maximum P300 probability. For P300-based word spellers, each round of flashing shown in Fig. 1 is composed of six row-flashing and six column-flashing. We therefore create two P300 probability vectors Φ^{row} and Φ^{col} of dimension six each to store the P300 probability (i.e., g'_1) of EEG trials extracted during the six row-flashing and six column-flashing (within one particular flashing round), respectively. As P300-based word spellers usually implement multiple rounds of flashing for the spelling of a single character, we identify the row-flashing and the column-flashing (EEG trials with P300) that specify the focused cell as follows:

$$\begin{aligned} \text{row}_{P300} &= \underset{i}{\text{argmax}} \sum_{j=1}^{R} \Phi_{i,j}^{\text{row}} \\ \text{col}_{P300} &= \underset{i}{\text{argmax}} \sum_{j=1}^{R} \Phi_{i,j}^{\text{col}} \end{aligned} \quad (9)$$

where parameter R denotes the number of flashing rounds implemented for the spelling of a single character, which is set at 10 in our setup (to be described in Section III-A). $\Phi_{i,j}^{\text{row}}$ and $\Phi_{i,j}^{\text{col}}, i = 1, \ldots, 6, j = 1, \ldots, R$ denote the two P300 probability vectors. In particular, subscript i changes from 1 to 6, indicating the number of the row-flashing and the column-flashing, respectively. Subscript $j, i = 1, \ldots, R$ denotes the round of flashing instead.

B. Subject-Independent EEG Modeling and Classification

Though many studies [19]–[21] have shown that P300 varies across subjects, different subjects usually share common waveform characteristics within their P300 as illustrated in Fig. 2. Therefore, compared with a subject model learned from EEG of any other specific subject, a classification model (SICM) learned from EEG of a pool of subjects is more capable of capturing such common waveform characteristics and accordingly should be more capable of classifying EEG of a new subject without the user calibration.

The idea of the subject-independent EEG modeling and classification is quite simple. First, we have a large amount of EEG collected from many previous subjects (EEG of a new subject to be studied is not included here) and the corresponding labels as follows:

$$\begin{aligned} X_p &= \{X_{s1}^T, \ldots, X_{si}^T, \ldots, X_{sn}^T\} \\ L_p &= \{L_{s1}^T, \ldots, L_{si}^T, \ldots, L_{sn}^T\} \end{aligned} \quad (10)$$

where X_{si} and L_{si} refer to EEG feature vectors converted from EEG of the ith subject and the corresponding label vector, respectively. In particular, each element of a label vector is equal to 1 or 2 to indicate the mode of EEG trial with or without P300, respectively. With the pooled subject EEG X_p and the corresponding labels L_p, the Gaussian distribution $p(X|\pi_c)$, $c = 1, 2$ in (7) can be estimated and a SICM can accordingly be built as described in Section II-A. Experiments (to be described in Section III-C) show that SICMs significantly outperform the cross-subject model learned from EEG of a single previous subject.

C. Adaptive EEG Modeling and Classification

This section presents the adaptive EEG modeling and classification technique. The SICM in the last subsection is capable of classifying EEG of a new subject with no user calibration. However, the classification accuracy is usually much lower than the SSSCM accuracy. The lower accuracy can be explained by the fact that SICMs capture the common instead of subject-specific P300 waveform characteristics.

One direct solution to compensate the deficiency of the SICM described above is to build a model that captures the subject-specific EEG characteristics. Different from the traditional user calibration approach, we build such model through an online adaptation process as follows. Given labeled EEG of a pool of previous subjects and a new subject to be studied, EEG recorded from the new subject is first classified by the SICM online at the initial adaptation stage. An ASSCM is then built by learning from the just classified subject EEG and the corresponding labels predicted by the SICM. After that, the ASSCM is iteratively

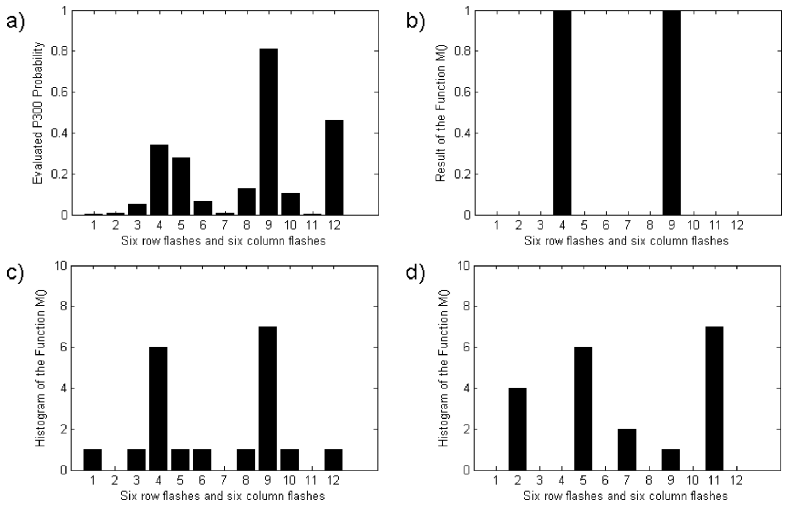

Fig. 4. Evaluation of the proposed EEG classification confidence score: (a) P300 probability of EEG trials extracted during 12 flashes within one flashing round; (b) Results of the function $f_m()$ in (11); (c) Histogram of $f_m()$ accumulated over 10 rounds of flashing; (d) Another histogram of $f_m()$ accumulated over another 10 rounds of flashing.

updated by incorporating the ensuing EEG of the new subject and the corresponding labels predicted by either the SICM or the ASSCM itself, depending on its confidence score. Algorithm I below describes the proposed online model adaptation technique step by step.

Algorithm I:

Input: Labeled EEG from many previous subjects and a new subject to be studied

Output: An ASSCM that is capable of classifying EEG of the new subject plus the classification results of the subject EEG that is used for the online adaptation.

Step 1) Preprocess the pooled subject EEG X_p and convert it into a set of EEG feature vectors. Build a label vector L_p corresponding to the converted EEG feature vectors.

Step 2) Train a SICM by learning from the labeled EEG feature vectors specified in Step 1.

Step 3) Preprocess and convert the initial EEG segment (EEG trials extracted during the twenty rounds of flashing that are used to spell the first two characters) from the new subject into EEG feature vectors X_1. Then classify X_1 by using the SICM built in Step 2.

Step 4) Build an ASSCM based on X_1 and the corresponding labels L_1 that are predicted by the SICM in Step 3.

Step 5) Preprocess and convert the ensuing EEG segments (EEG trials extracted during the ten rounds of flashing used to spell a character) of the new subject into EEG feature vectors X_i. Classify X_i by both the SICM and the ASSCM. Determine the labels of X_i (i.e., L_i) by either the SICM or the ASSCM, depending on a confidence score defined in (11).

Step 6) Update the ASSCM by using a subset of EEG segments $X_1, \ldots, X_i$ classified so far and the corresponding labels determined in Step 3 and Step 5.

Step 7) Repeat Steps 5 and 6 until a certain amount of EEG of the new subject has been adapted.

In Step 5 of Algorithm I, a confidence score is required to select the SICM and the ASSCM when they are applied to predict the labels of the next EEG segment. Besides, a confidence score is also needed in Step 6 to select a subset of the classified subject EEG. In the proposed technique, both confidence scores are evaluated based on the model's EEG classification consistency defined as follows:

$$C = f_p\left(\sum_{j=1}^{R} f_m(\Phi_j^{\text{row}})\right) - f_{sp}\left(\sum_{j=1}^{R} f_m(\Phi_j^{\text{row}})\right) + f_p\left(\sum_{j=1}^{R} f_m(\Phi_j^{\text{col}})\right) - f_{sp}\left(\sum_{j=1}^{R} f_m(\Phi_j^{\text{col}})\right) \quad (11)$$

where R represents the number of the flashing rounds for the spelling of a character. Φ_j^{row} and Φ_j^{col} denote the row and the column P300 probability vectors of EEG trials extracted during the jth round of flashing, respectively. Function $f_m()$ returns a 6-D vector that sets the row or column with the maximum P300 probability at 1 and the rest at 0 as illustrated in Fig. 4(b). Functions $f_p()$ and $f_{sp}()$ return the peak and second-peak frequency of the row and column with the maximum P300 probability (accumulated over R rounds of flashing), respectively, as illustrated in Fig. 4(c) and (d).

As (11) shows, the confidence score is actually evaluated according to its classification consistency. Such evaluation is based on the observation that EEG with P300 shows specific pattern but those without P300 are much more random. In particular, a model's confidence score will be high when 1) the peak frequency of the row/column with the maximum P300 probability is high and 2) the difference between the peak and the second-peak frequency is high. The second requirement ensures the saliency of the peak frequency of the row/column with the maximum P300 probability.

Fig. 4 further illustrates how the confidence score is evaluated in (11). Particularly, Fig. 4(a) shows the P300 probability of the 12 flashes within one specific flashing round. Fig. 4(b) shows the results of the function $f_m()$ in (11). Fig. 4(c) shows the frequency of the row and the column with the maximum P300 probability that is accumulated over 10 rounds of flashing. Clearly, the peak/second-peak frequencies of the row-flashing and column-flashing reach up to 6/1 and 7/1, respectively. The confidence score can therefore be evaluated at 11 (i.e., $6-1+7-1$). But for another ten rounds of flashing shown in Fig. 4(d), though the peak and second-peak frequencies are the same as that in Fig. 4(c), the confidence score is just evaluated as 7 (i.e., $6-4+7-2$) because of the lower saliency of the peak frequency.

Consequently, the label of the ensuing EEG segment of the new subject can be uniformly determined based on confidence scores of the SICM and the ASSCM as follows:

$$L = \begin{cases} L_{\mathrm{SICM}}, & \text{if } C_{\mathrm{SICM}} \geq C_{\mathrm{ASSCM}} \\ L_{\mathrm{ASSCM}}, & \text{otherwise} \end{cases} \tag{12}$$

where C_{SICM} and C_{ASSCM} refer to confidence scores of the SICM and the ASSCM, respectively. L_{SICM} and L_{ASSCM} refer to the label predicted by using the SICM and the ASSCM, respectively. Clearly, the label of the ensuing subject EEG segment is determined by the model (either the SICM or the ASSCM) with a higher confidence score.

As described in Algorithm I, the proposed technique derives an ASSCM through an online adaptation process, which is actually very similar to the semi-supervised learning that is often used while only a small amount of labeled training data is available [8]. However, the proposed technique requires no labeled EEG of the new subject compared with the semi-supervised learning. Instead it uses a SICM (learned from EEG of a pool of previous subjects offline) as a seed model to make an initial label prediction. At the same time, as the SICM is capable of achieving pretty high EEG classification accuracy shown in Fig. 6 (to be discussed in Section III-D), the proposed technique is capable of classifying EEG accurately even at the very initial adaptation stage (when the ASSCM suffers from under-fitting severely).

It should be noted that we do not use all classified subject EEG to update the ASSCM as described in Algorithm I. In particular, we update the ASSCM by using 80% most confident subject EEG classified so far. The use of 80% most confident subject EEG is based on the observation that the accuracy of SICMs shown in Fig. 6 is usually higher than 80% and the accuracy of the ASSCM also surpasses 80% quickly after around 30–50 rounds of online adaptation. Therefore, the labels of the 80% most confident subject EEG should be pretty accurate, though they may not be perfect accurate. In addition, the accuracy of the ASSCM saturates and converges to that of the SSSCM after around 200 rounds of subject EEG are adapted online shown in Fig. 6. Therefore, 300–400 rounds of online adaptation should be enough to derive a stable ASSCM as stated in Step 7 in Algorithm I.

III. Experimental Results

The proposed EEG modeling and classification technique is evaluated in this section. First, data collection from a P300-based word speller is briefly described. After that, P300 variations across subjects are studied based on the performance of the cross-subject EEG classification. Lastly, the proposed subject-independent and adaptive EEG modeling and classification techniques are evaluated extensively based on the collected EEG data.

A. Data Collection

The proposed EEG classification technique is tested over a P300-based word speller reported in our earlier work [16]. In that speller system, subject EEG is first amplified by a Neuroscan amplifier called SynAmps2 and then piped to a server by the Neuroscan software. The SynAmpls2 has 64 monopolar channels and we just use eight channels that are proposed in [30]. In particular, the work in [30] tests different channel sets and finds that the combination of three classical channels (i.e., Fz, Cz, Pz) and five channels at the posterior region (i.e., PO7, PO8, OZ, P3, P4) produces the best classification performance.

During the EEG collection stage, subjects sit in front of a 6×6 matrix of characters shown in Fig. 1 where the six rows and columns flash alternatively in a random order. Subjects need to focus on one specific cell visually during each flashing round (defined by the flashing of the six rows and six columns one time). When a particular row or column flashes, a corresponding stimulus code is generated in a time-locked fashion, which divides the collected EEG into epoch of 500 ms starting from the time of stimulus onset. Therefore, one row flash and one column flash within each flashing round indicate the focused cell, which can be determined through the identification of the P300 from the recorded EEG.

In our study, EEG of ten healthy subjects is collected by using the P300-based word spell described above. For each subject, two EEG sessions are collected sequentially, which correspond to the spelling of the same set of 41 characters "THE QUICK BROWN FOX JUMPS OVER LAZY DOG 246138 579" two times but in different orders in each time. In particular, ten rounds of flashing are implemented for the spelling of each character and EEG between 150 and 500 ms after the onset of each flash is used for the EEG classification. Throughout our experiments, we evaluate the proposed techniques by using the two EEG sessions collected from each of the ten healthy subjects under study.

B. Intersubject EEG Variance

We study P300 variations through the examination of the performance of the cross-subject EEG classification. Particularly, ten SSSCMs are first built by learning from the first EEG session (or the second session for two-fold cross validation) of the ten healthy subjects, which are then applied to classify the second EEG session (or the first) of the ten healthy subjects, respectively. Table I shows the EEG classification accuracy that is defined by the fraction of EEG samples correctly classified. In particular, the first row and the first column show the testing and training EEG of the ten healthy subjects, respectively. Therefore, the diagonal items actually show the SSSCM accuracy, which is evaluated by using the classification models learned from the subjects' own EEG. On the other hand, the

TABLE I
ACCURACY (FRACTION OF EEG SAMPLES CORRECTLY CLASSIFIED) OF CROSS-SUBJECT EEG CLASSIFICATION

Training data \ Testing data	Subj. 1	Subj. 2	Subj. 3	Subj. 4	Subj. 5	Subj. 6	Subj. 7	Subj. 8	Subj. 9	Subj. 10
Subj. 1	0.99	0.80	0.93	0.87	0.41	0.83	0.72	0.70	0.85	0.48
Subj. 2	0.90	0.98	0.83	0.59	0.29	0.48	0.37	0.40	0.84	0.43
Subj. 3	0.91	0.73	0.99	0.85	0.26	0.84	0.63	0.71	0.68	0.63
Subj. 4	0.78	0.46	0.77	1.00	0.40	0.89	0.60	0.49	0.88	0.37
Subj. 5	0.49	0.28	0.50	0.63	0.90	0.68	0.52	0.67	0.40	0.17
Subj. 6	0.59	0.17	0.66	0.87	0.40	1.00	0.95	0.96	0.68	0.20
Subj. 7	0.55	0.28	0.66	0.88	0.37	0.85	1.00	0.88	0.66	0.23
Subj. 8	0.24	0.21	0.44	0.50	0.11	0.89	0.66	1.00	0.21	0.30
Subj. 9	0.89	0.89	0.90	0.99	0.54	0.93	0.83	0.82	1.00	0.52
Subj. 10	0.84	0.62	0.72	0.52	0.15	0.54	0.62	0.78	0.56	0.95

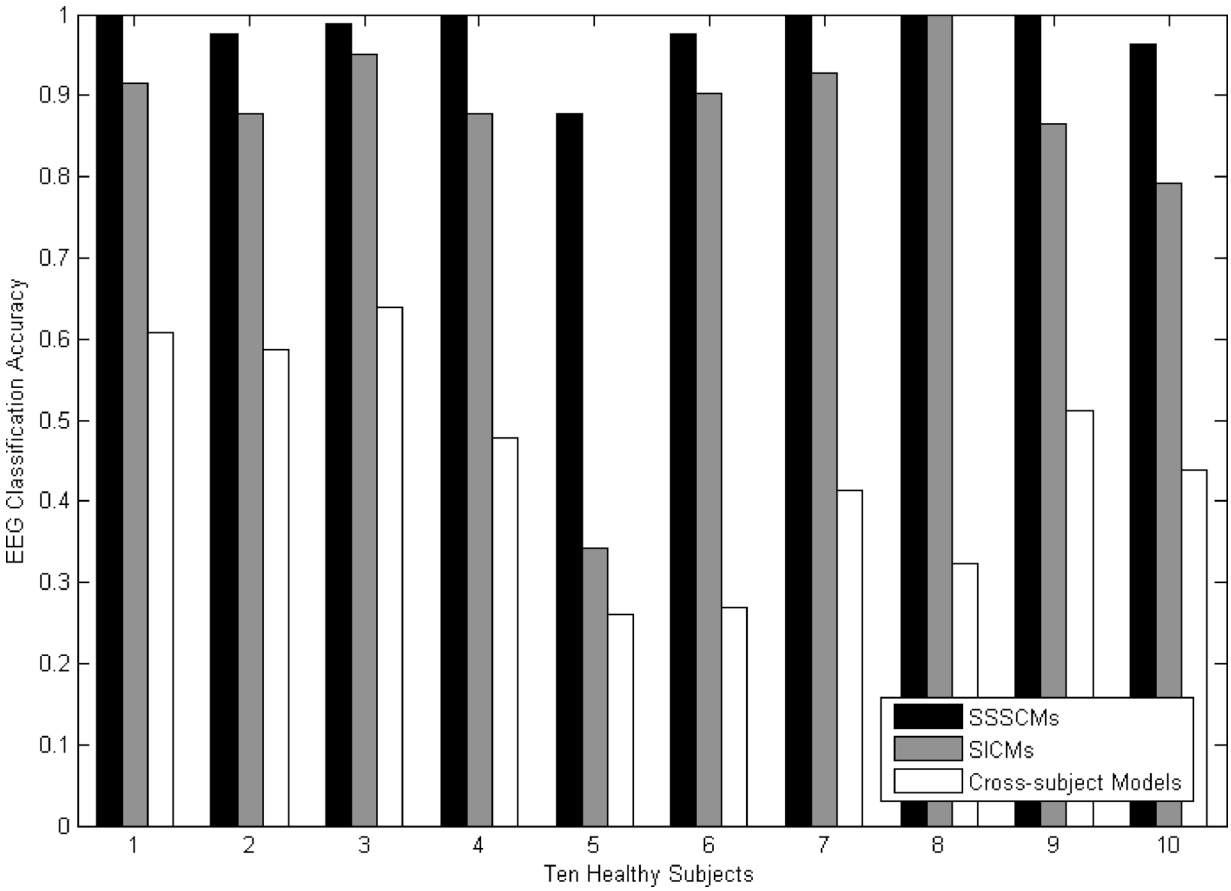

Fig. 5. Accuracy of SSSCMs (black bars), SICMs (gray bars), and cross-subject models (white bars): The accuracy is evaluated through the two-fold cross validation over the two EEG sessions that are collected from the ten healthy subjects described in Section III-A. The accuracy of cross-subject models (white bars) is evaluated by averaging the nondiagonal items in Table I column by column.

nondiagonal items show the cross-subject model accuracy, which is evaluated by the classification models learned from EEG of other subjects.

Fig. 5 further compares the accuracy of the subject-specific and cross-subject EEG classification models of the ten subjects under study. In particular, for each subject the black bar on the left shows the SSSCM accuracy. The white bar on the right instead shows the cross-subject model accuracy that is evaluated by averaging the nondiagonal items in Table I column by column. As Fig. 5 shows, the cross-subject model accuracy is significantly lower than the SSSCM accuracy, indicating the EEG variations across subjects.

C. Subject-Independent EEG Modeling and Classification

The subject-independent EEG modeling and classification technique has also been tested. For each of the ten healthy subjects, a SICM is first built by learning from the first EEG session (or the second for two-fold cross validation) collected from the other nine subjects. The trained SICM is then applied to classify the second EEG session (or the first session) of the subject under study.

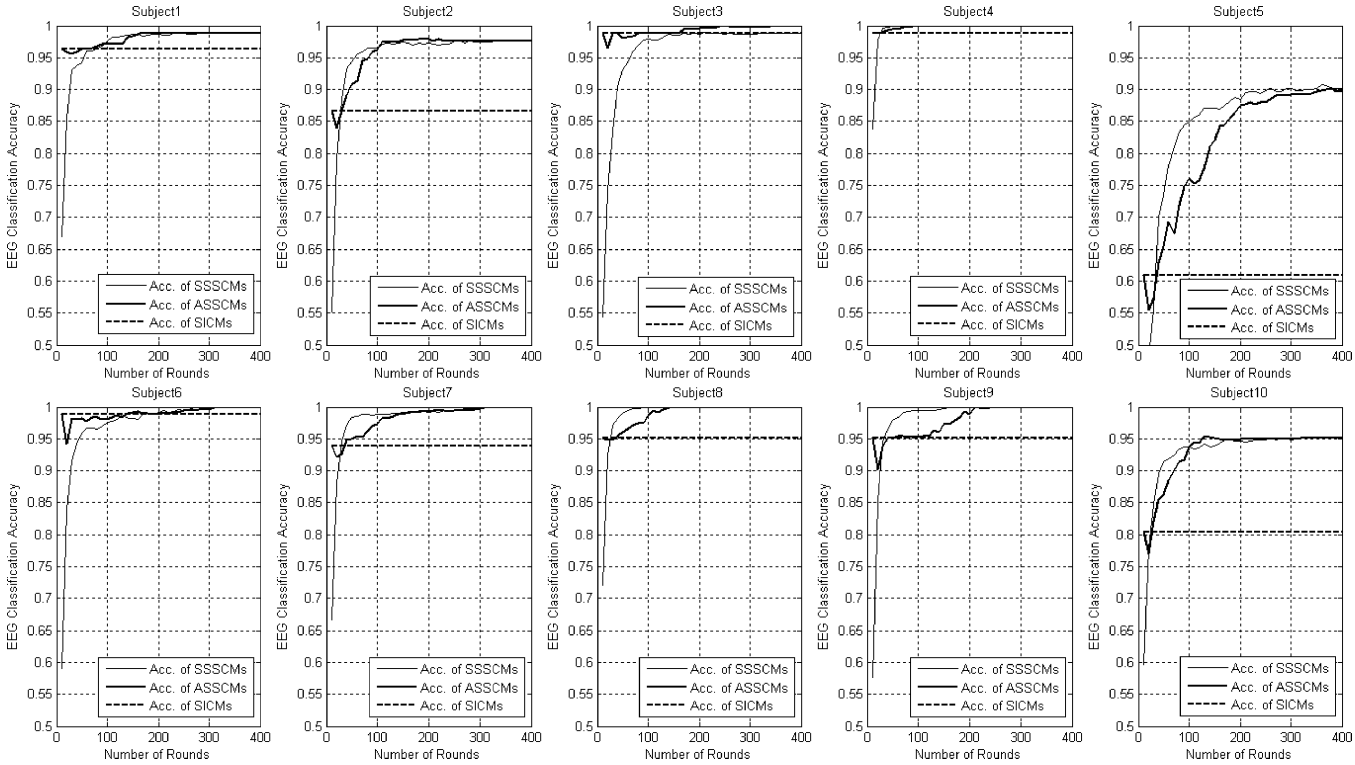

Fig. 6. Accuracy of SICMs (dashed graph), ASSCMs (solid heavy dark graph), and SSSCMs (solid light dark graph). The accuracy of the SICMs does not change with respect to the online adaptation process, while the accuracy of the SSSCMs and ASSCMs increases when more labeled and unlabeled EEG of the new subject is adapted online. It should be noted that the spelling of each character requires ten rounds of flashing.

The gray bars in Fig. 5 show the SICM accuracy of the ten subjects under study. As Fig. 5 shows, the SICM accuracy is generally much higher than the cross-subject model accuracy. Such results indicate that the use of the pooled EEG does improve the EEG classification performance greatly. On the other hand, the SICM accuracy is normally more or less lower than the SSSCM accuracy. In particular, the SICM accuracy may be significantly lower than the SSSCM accuracy for some specific subjects (i.e., the second, fifth, and tenth subjects). Such results concurrently indicate the limitation of SICMs, i.e., they capture the common instead of the subject-specific P300 waveform characteristics.

D. Adaptive EEG Modeling and Classification

The adaptive EEG modeling and classification technique has been evaluated extensively. To remove the possible effect of the EEG collection order, we first randomly sort the 41 characters in one session and then segment the sorted characters into 40 segments including two characters in the first segment and 1 in each of the remaining 39 segments. In addition, ten rounds of the random EEG sorting and segmentation described above are implemented for each of the two EEG sessions (the other session will be used as the testing data as a whole). It should be noted that the use of two characters in the first EEG segment is to avoid the singularity of the covariance matrix that need to be evaluated in (7).

Considering the two-fold cross validation and the ten rounds of EEG sorting and segmentation, 20 sets of ASSCMs (i.e., 2×10) are built for each subject where each set is composed of 40 ASSCMs. In addition, 20 sets of SSSCMs (40 in each set as well) are also built based on the 20 sets of sorted and segmented subject EEG. In particular, the ith SSSCM in each set is built by learning from the first i segments of the labeled subject EEG. The accuracy of the two groups of SSCMs is evaluated by applying them to the other EEG session of the ten subjects under study.

Fig. 6 shows EEG classification accuracy averaged over the 20 sets of SSSCMs and ASSCMs, respectively. As Fig. 6 shows, the adaptation process can be divided into three stages where the first stage refers to the initial adaptation period (around the first 30 rounds of EEG). In this stage, ASSCM accuracy is significantly higher than SSSCM accuracy when SSSCMs suffer from under-fitting severely. The higher ASSCM accuracy can be explained by SICMs that determine the EEG label because of their higher confidence score shown in Fig. 7. The second stage corresponds to 30–200 rounds of online adaptation shown in Fig. 6. In this stage, SSSCM accuracy surpasses ASSCM accuracy because of error of EEG labels predicted by either SICMs or ASSCMs themselves. The third stage corresponds to 200–400 rounds of online adaptation. In this stage, ASSCM accuracy converges to SSSCM accuracy, indicating the stability of the proposed method.

Fig. 7 shows the averaged confidence scores of SICMs and ASSCMs, respectively. As SICMs are fixed during the model adaptation process, SICM confidence scores (labeled by heavy dark graph) vary within a small range throughout the online adaptation procedure. In addition, ASSCM confidence scores

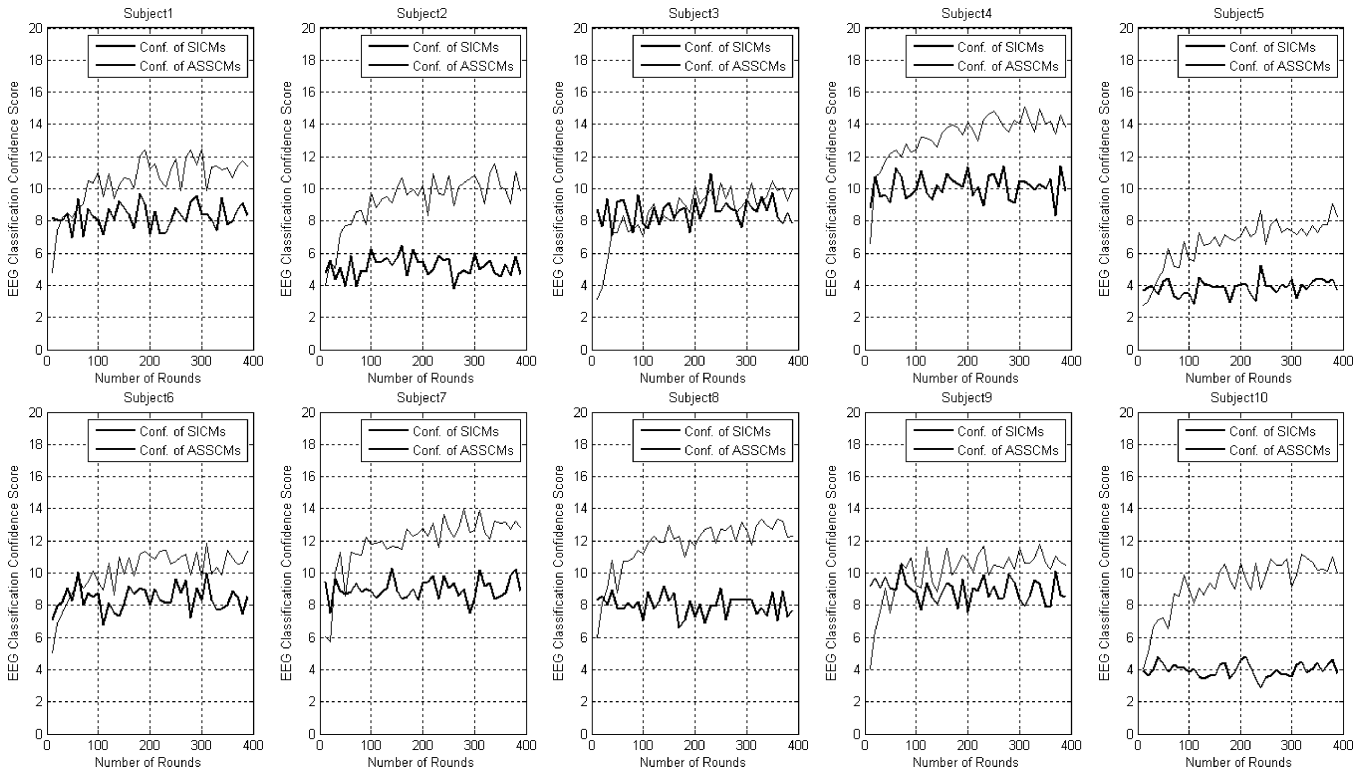

Fig. 7. Confidence score of SICMs (solid heavy graph) and ASSCMs (solid light graph). The confidence score of SICMs is stable because SICMs are fixed during the online adaptation process. But the confidence score of ASSCMs increases steadily when more subject EEG is adapted. It should be noted that the spelling of each character requires ten rounds of flashing.

(labeled by light dark graph) are normally lower than SICM confidence scores at the early adaptation stage. However, they increase and surpass SICM confidence scores quickly after a small amount of subject EEG is adapted online. It should be noted that ASSCM confidence scores in Fig. 7 are averaged over the 20 sets of ASSCMs described above. For different sets of ASSCMs, their confidence scores may surpass SICM confidence scores at different points.

In addition, Fig. 8 further shows the accuracy standard deviation of the 20 sets of ASSCMs and SSSCMs described above. In particular, for each subject the light gray and the heavy graph show the accuracy standard deviation of the SSSCM and the ASSCM, respectively. As Fig. 8 shows, the accuracy standard deviation of ASSCMs consistently converges to that of SSSCMs. Such results also indicate the stability of the proposed online adaptation technique.

IV. Discussion

Compared with SSSCMs, SICMs and ASSCMs both remove the traditional user calibration procedure. In addition, ASSCMs are capable of achieving virtually the same performance as SSSCMs after a small amount of subject EEG (100–200 rounds) is adapted online. Furthermore, subject EEG used for the online adaptation is also classified accurately. For the 20 sets of ASSCMs of each subject described in Section III-C, the accuracy of EEG of the ten subjects (used for the online adaptation) reaches up to 84.77%–96.19%. This property enables users to use P300-based word spellers directly without the user calibration. It also explains the stable performance improvement of ASSCMs and their quick convergence to SSSCMs as illustrated in Fig. 6.

Several issues need to be further investigated. First, it should be noted that a certain number of subjects have no evident P300 and so cannot use P300-based word spellers even after a traditional user calibration. For these subjects, the proposed technique cannot adapt a good ASSCM either. Second, for disabled subjects, P300 may not be detected from the eight selected channels properly. Under such circumstance, automatic online channel selection should be studied to identify subject-specific channels with evident P300. Third, the proposed technique is solely evaluated over ten healthy subjects. But for people from a more diverse population, a higher degree of EEG variations can be expected, which may prolong the online adaptation process more or less, depending on the degree of the EEG variations. One possible solution to this problem is to build multiple category-specific SICMs. Then for a new user, a category-specific SICM can be selected based on the category of the new user. Fourth, the proposed technique is only evaluated by a P300-based word speller. But the ideas of learning a SICM from a pool of subjects and the iterative online adaptation from a SICM to an ASSCM have potentials to be applied to other BCI tasks such as motor imagery. We will further study these issues in our future work.

V. Conclusion

This paper presents an unsupervised EEG modeling and classification technique and its applications to P300-based word

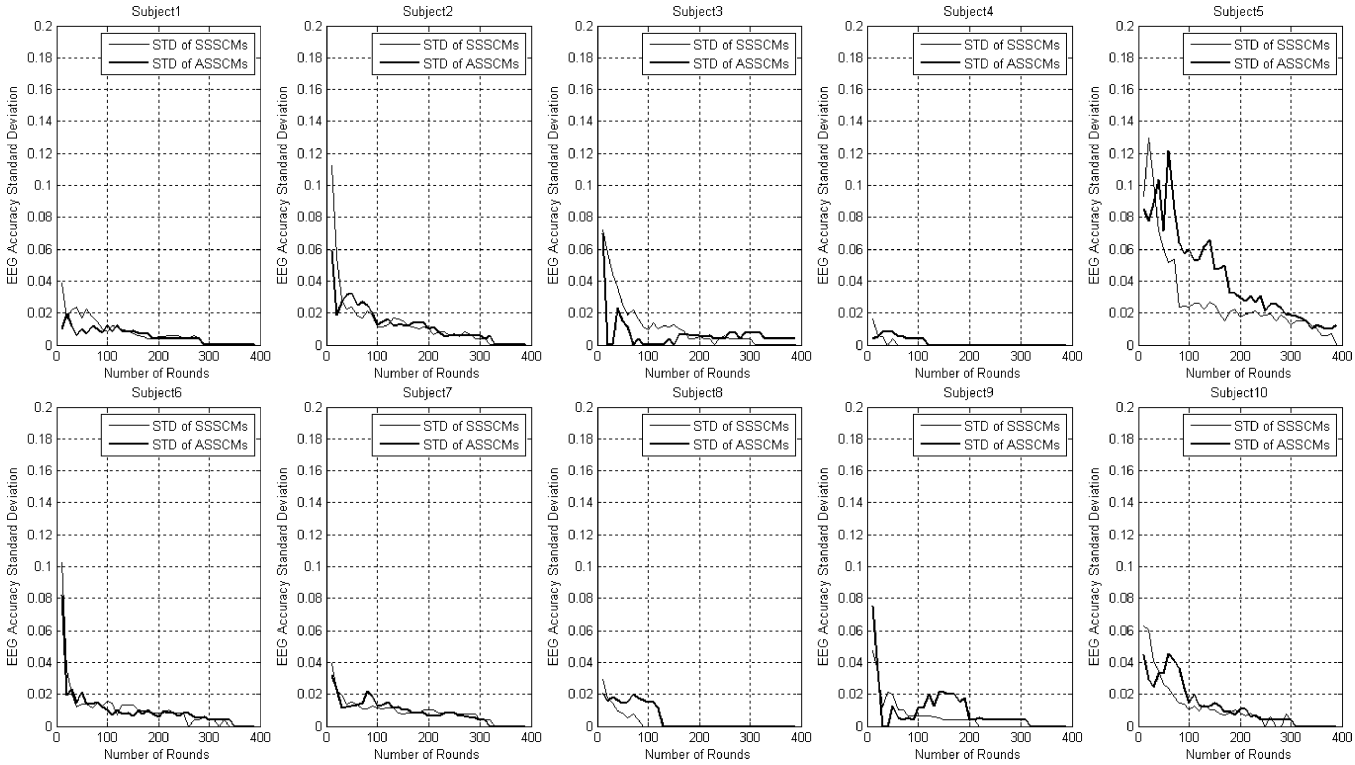

Fig. 8. Accuracy standard deviation of ASSCMs (solid heavy graph) and SSSCMs (solid light graph). The standard deviation of ASSCMS is very small and converges to that of SSSCMs when more subject EEG is used for the model adaptation. It should be noted that the spelling of each character requires ten rounds of flashing.

spellers. In the proposed technique, a SICM is first built by learning from EEG of a pool of subjects, which captures the common P300 characteristics and greatly outperforms the subject model learned from EEG of one specific subject. Starting from a SICM, an ASSCM is then adapted online for a new subject through an iterative adaptation procedure. Experiments over ten healthy subjects show that the ASSCM is capable of achieving virtually the same performance as the SSSCM. This indicates that it is feasible to avoid the traditional user calibration procedure and accordingly making P300-based BCIs more convenient for practical uses.

REFERENCES

[1] J. R. Wolpaw, N. Birbaumer, D. J. McFarland, G. Pfurtscheller, and T. M. Vaughan, "Brain-computer interfaces for communication and control," *Clin. Neurophysiol.*, vol. 113, no. 6, pp. 767–791, 2002.

[2] E. A. Curran and M. J. Strokes, "Learning to control brain activity: A review of the production and control of EEG components for driving brain-computer interface (BCI) systems," *Brain Cognit.*, vol. 51, no. 3, pp. 326–336, 2003.

[3] S. P. Levine, J. E. Huggins, S. L. BeMent, R. K. Kushwaha, L. A. Schuh, M. M. Rohde, E. A. Passaro, D. A. Ross, K. V. Elisevich, and B. J. Smith, "A direct brain interface based on event-related potentials," *IEEE Trans. Neural Syst. Rehabil. Eng.*, vol. 8, no. 2, pp. 180–185, Jun. 2000.

[4] M. A. Lebedev and M. A. L. Nicolelis, "Brain-machine interfaces: Past, present and future," *Trends Neurosci.*, vol. 29, no. 9, pp. 536–546, 2006.

[5] J. R. Wolpaw and D. J. McFarland, "Multichannel EEG-based brain-computer communication," *Electroencephalograp. Clin. Neurophysiol.*, vol. 90, no. 6, pp. 444–449, 1994.

[6] B. Blankertz, G. Dornhege, C. Schafer, R. Krepki, J. Kohlmorgen, K. R. Mueller, V. Kunzmann, F. Losch, and G. Curio, "Boosting bit rates and error detection for the classification of fast-paced motor commands based on single-trial EEG analysis," *IEEE Trans. Neural Syst. Rehabil. Eng.*, vol. 11, no. 2, pp. 127–131, Jun. 2003.

[7] N. Xu, X. Gao, B. Hong, X. Miao, S. Gao, and F. Yang, "BCI competition 2003—Data set IIb: Enhancing P300 wave detection using ICA-based subspace projections for BCI applications," *IEEE Trans. Biomed. Eng.*, vol. 51, no. 6, pp. 1067–1072, Jun. 2004.

[8] Y. Li and C. Guan, "Joint feature re-extraction and classification using an iterative semi-supervised support vector machine algorithm," *Mach. Learn.*, vol. 71, no. 1, pp. 33–53, 2008.

[9] Y. Li, H. Li, C. Guan, and Z. Y. Chin, "An self-training semi-supervised SVM algorithm and its application in an EEG-based brain computer interface speller system," *Pattern Recognit. Lett.*, vol. 29, no. 9, pp. 1285–1294, 2008.

[10] S. Lu, C. Guan, and H. Zhang, "Learning adaptive subject-independent P300 models for EEG-based brain-computer interfaces," in *Int. Joint Conf. Neural Networks*, 2008, pp. 2462–2466.

[11] J. F. Borisoff, S. G. Mason, and G. E. Birch, "Brain interface research for asynchronous control applications," *IEEE Trans. Neural Syst. Rehabil. Eng.*, vol. 14, no. 2, pp. 160–164, Jun. 2006.

[12] E. Halgren, K. Marinkovic, and P. Chauvel, "Generators of the late cognitive potentials in auditory and visual oddball tasks," *Electroencephalogr. Clin. Neurophysiol.*, vol. 106, no. 2, pp. 156–164, 1998.

[13] L. A. Farwell and E. Donchin, "Talking off the top of your head: Toward a mental prosthesis utilizing event-related brain potential," *Electroencephalogr. Clin. Neurophysiol.*, vol. 70, no. 6, pp. 510–523, 1988.

[14] H. Serby, E. Yom-Tov, and G. F. Inbar, "An improved P300-based brain-computer interface," *IEEE Trans. Neural Syst. Rehabil. Eng.*, vol. 13, no. 1, pp. 89–98, Mar. 2005.

[15] E. Donchin, K. M. Spencer, and R. Wijesinghe, "The mental prosthesis: Assessing the speed of a P300-based brain-computer interface," *IEEE Trans. Rehabil. Eng.*, vol. 8, no. 2, pp. 174–179, Jun. 2000.

[16] T. Manoj, C. Guan, and J. Wu, "Robust classification of EEG signal for brain-computer interface," *IEEE Trans. Neural Syst. Rehabil. Eng.*, vol. 14, no. 1, pp. 24–29, Mar. 2006.

[17] H. Zhang, C. Guan, and C. Wang, "Towards asynchronous P300-based brain-computer interfaces: A computational approach with statistical models," *IEEE Trans. Biomed. Eng.*, vol. 55, no. 6, pp. 1754–1763, Jun. 2008.

[18] M. Kaper, P. Meinicke, U. Grossekathoefer, T. Lingner, and H. Ritter, "Support vector machines for the p300 speller paradigm," *IEEE Trans. Biomed. Eng.*, vol. 51, no. 6, pp. 1073–1076, Jun. 2004.

[19] N. Noldy, R. Stelmack, and K. Campbell, "Event-related potentials and recognition memory for pictures and words: The effects of intentional and incidental learning," *Psychophysiology*, vol. 27, no. 4, pp. 417–428, 1990.
[20] R. Emmerson, R. Dustman, D. Shearer, and C. Turner, "P300 latency and symbol digit performance correlations in aging," *Exp. Aging Res.*, vol. 15, no. 3–4, pp. 151–159, 1990.
[21] M. Kutas, G. McCarthy, and E. Donchin, "Augmenting mental chronometry: The p300 as a measure of stimulus evaluation time," *Science*, vol. 197, no. 4305, pp. 792–795, 1977.
[22] J. Polich, "On the relationship between EEG and P300: Individual differences, aging, and ultradian rhythms," *Int. J. Psychophysiol.*, vol. 26, no. 1, pp. 299–317, 1997.
[23] T. M. Vaughan, "Guest editorial brain-computer interface technology: A review of the second international meeting," *IEEE Trans. Neural Syst. Rehabil. Eng.*, vol. 11, no. 2, pp. 94–109, Jun. 2003.
[24] C. Guan, X. Zhu, S. Ranganatha, M. Thulasidas, and J. Wu, "Robust classification of event-related potential for brain-computer interface," in *Int. Conf. Adv. Med. Signal Inf. Process.*, 2004, pp. 321–326.
[25] M. Thulasidas, C. Guan, S. Ranganatha, J. Wu, X. Zhu, and W. Xu, "Effect of ocular artifact removal in brain computer interface accuracy," in *Proc. 26th IEEE Int. Conf. Eng. Med. Biol. Soc.*, 2004, vol. 6, pp. 4385–4388.
[26] S. M. Haas, M. G. Frei, I. Osorio, B. Pasik-Duncan, and J. Radel, "EEG ocular artifact removal through ARMAX model system identification using extended least squares," *Commun. Inf. Syst.*, vol. 3, no. 1, pp. 19–40, 2003.
[27] D. J. Krusienski, E. W. Sellers, F. Cabestaing, S. Bayoudh, D. J. McFarland, T. M. Vaughan, and J. R. Wolpaw, "A comparison of classification techniques for the P300 speller," *J. Neural Eng.*, vol. 3, no. 34, pp. 299–305, 2006.
[28] B. D. Ripley, *Pattern Recognition and Neural Networks*. Cambridge, U.K.: Cambridge Univ. Press, 1996.
[29] R. O. Duda, P. E. Hart, and D. G. Stork, *Pattern Classification*, 2nd ed. New York: Wiley, 2000.
[30] D. J. Krusienski, E. W. Sellers, D. J. McFarland, T. M. Vaughan, and J. R. Wolpaw, "Toward enhanced P300 speller performance," *J. Neurosci. Methods*, vol. 167, no. 1, pp. 15–21, 2007.

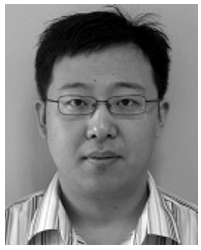

Shijian Lu (M'07) received the Ph.D. degree in electrical and computer engineering from National University of Singapore, in 2005.

Currently, he is a Research Fellow in the Institute for Infocomm Research, Agency for Science, Technology and Research, Singapore. His current research interests include brain–computer interface, pattern recognition, machine learning, and medical image processing. He has published over 30 peer-reviewed journal and conference papers.

Cuntai Guan (M'97–SM'03) received the Ph.D. degree in electrical and electronic engineering from Southeast University, Nanjing, China, in 1993.

He established the Brain–Computer Interface Group at Institute for Infocomm Research, Agency for Science, Technology and Research (A*STAR), Singapore, where he is currently a Senior Scientist and a Program Manager. His current research interests include brain–computer interface, neural signal processing, machine learning, pattern classification, and statistical signal processing, with applications to assistive device, rehabilitation, and health monitoring. He has published over 70 peer-reviewed journal and conference papers.

Dr. Guan is the President of Pattern Recognition and Machine Intelligence Association, Singapore.

Haihong Zhang received the Ph.D. degree in computer science from National University of Singapore, in 2005.

Thereafter he joined the Institute for Infocomm Research in Singapore as a research fellow. He is now a project manager for neural signal processing, where his research interests include machine learning, pattern recognition, and brain signal processing for high performance brain–computer interfaces.